Physical and Biological Modeling of a 100 Megawatt Ocean Thermal Energy Conversion Discharge Plume

Greg J. Rocheleau and Patrick Grandelli (P.E.)
Makai Ocean Engineering, Inc.
P.O. Box 1206
Kailua, Hawai`i 96734
www.makai.com (808) 259-8871

Abstract—A numerical model has been developed to rigorously simulate the physical oceanographic effects of one or several 100 megawatt Ocean Thermal Energy Conversion (OTEC) plant(s). The model suggests that OTEC plants can be configured such that the plant can conduct continuous operations, with resulting temperature and nutrient perturbations that are within naturally occurring levels. This presentation will describe the development and results of the numerical model, focusing on the physical and biological effects of operating single and multiple 100 megawatt OTEC plants in Hawaiian waters, and will discuss the implications of these results towards future design and regulatory work. Detailed statistics and visualization of the thermal variation, plume dilution, and estimates of the biological growth around an OTEC plant will be presented. Studies to date suggest that by discharging the OTEC flows downwards at a depth below 70 meters, the dilution is adequate and nutrient enrichment is small enough so that 100 megawatt OTEC plants could be operated in a sustainable manner on a continuous basis.

Keywords-OTEC; plume; model; thermal; discharge; EFDC; Hawaii Regional Ocean Model; ocean thermal energy conversion; marine renewable energy

I. INTRODUCTION

Ocean Thermal Energy Conversion (OTEC) is a process that uses large quantities of deep cold seawater and warm surface seawater to drive a Rankine power cycle to generate electricity. Small OTEC systems have previously demonstrated OTEC's capability to produce continuous, utility-grade electricity. Recent advances in offshore technology have led to interest in developing floating OTEC facilities that are large enough to be commercially viable. Various OTEC technology projects are presently being undertaken by the Office of Naval Research, Naval Facilities Engineering Command, U.S. Department of Energy, and Lockheed Martin Corporation. The National Oceanic and Atmospheric Administration (NOAA) is reviewing OTEC regulations written during the 1980s.

This paper describes a hydrodynamic numerical model situated in Hawaiian waters that simulates the near-field and far-field dilution and circulation of the large volumes of seawater used by a commercial-size, 100 MW OTEC plant. One such facility requires approximately 420 cubic meters per second of warm (~26°C) shallow seawater and 320 cubic meters per second of deep seawater (~4°C) from 1000 meter depth. Quantifying the dilution and circulation of these flows as part of the platform design process will be needed to obtain the required discharge permits and to ensure the long-term sustainability of the OTEC plant. Supported by the Center of Excellence in Ocean Sciences (CEROS) and the U.S. Department of Energy, this new model is more complex and realistic than was computationally practical for similar studies performed three decades ago [1].

The open-ocean waters of Hawai'i are a stratified and oligotrophic system, with low nutrient concentrations in the mixed layer and increasing nutrient concentrations below the photic zone. As a result, the nutrient-rich deep water will cause OTEC discharges to have elevated nutrient concentrations compared to the surrounding ambient ocean, which may cause a biological response and increase in primary productivity of certain species [2]. Minimizing the effects of nutrient redistributions in the photic zone through sufficient dilution and depth of discharge is a significant question among designers and regulating agencies. In 2010, NOAA, the United States' licensing agency for OTEC, sponsored a workshop to help ensure that the development of commercial-scale OTEC facilities will be environmentally acceptable.

Finding an adequate and optimal discharge configuration to achieve plume dilution and depth required a new modeling tool capable of resolving the dynamic behavior of large scale OTEC discharges in realistic ocean conditions. In 2010 Makai developed a numerical model, the Makai OTEC Plume Model. We chose to use the three-dimensional, time-dependent model Environmental Fluid Dynamics Code [3]. EFDC is EPA-certified and has been used on hundreds of studies involving coastal and estuarine systems, and includes a coupled lagrangian plume model for turbulent thermal discharges. The EFDC computional domain receives boundary conditions from the Hawaii Regional Ocean Model operated by the University of Hawaii as part of the HiOOS system. The Hawaii Regional Ocean Model, a nested Regional Ocean Model System (ROMS), provides nowcasts and hindcasts to the state of Hawaii [4]. This ROMS model receives outer boundary conditions forced by the Pacific Navy Coastal Ocean Model, and assimilates local data from satellite sea-surface altimetry, local wind sensors, glider buoys, and current meters. Several months of data were selected from the ROMS hindcasts to represent baseline environmental conditions, including typical seasonal changes as well as extreme conditions that could alter the local circulation and plume properties, such as transient

0-933957-39-8 ©2011 MTS

mesoscale eddies. Results were visualized with Makai's 4D visualization software, *Makai Voyager*. Used in combination, these tools allow for engineers and regulators to consider the sustainability of a particular OTEC plant design, under varying and realistic environmental conditions. Work has also started on biological modeling to simulate the phytoplankton response to the dynamic nutrient loads, with support provided by the Department of Energy (DoE).

II. Model Methods

A. OTEC Plant Configuration

Fig. 1 shows an offshore floating OTEC plant with a 1000 meter deep intake pipeline pipeline. The 100 megawatt plant floating offshore will intake ~320 cubic meters per second of cold water from 1000 meter depth and 420 cubic meters per second of warm water are drawn in at 20 meter depth. These flows pass through the heat exchangers before being mixed and discharged vertically downward, some distance below the plant. Mixing the warm water discharge with cooler water causes both discharges to remain below the mixed layer, where the plume spreads out horizontally within a relatively thin constant density layer (where there is limited mixing across diapycnals). This significantly reduces the re-circulation of the cooled warm water back into the surface intake, and avoids degrading the thermal resources. The discharge flow is characterized by an initial jet-plume, dominated by momentum and buoyancy forces and diluted through shear and vortex entrainment.

At some point, after entraining the surrounding water, the jet-plumes reach a density equilbirium with the surroundings and have lost their initial momentum. The plumes then enter the far-field regime, largely remaining within a neutral density layer and becoming dispersed through ambient ocean turbulence. Modeling these range of flows under realistic conditions required software that resolved the plume in both the near-field momentum and buoyancy-driven phase and the far-field passive dispersion phase. To achieve this, the OTEC plume model uses a two-way coupling between a lagrangian plume model and the finite-difference EFDC domain.

B. Numerical Model

EFDC solves a three-dimensional, vertically hydrostatic, free surface, turbulent averaged equation of motion for a variable density fluid. It utilizes the Mellor-Yamada 2.5 closure scheme to provide an accurate parameterization of the turbulence, and recent model-data comparisons have shown that the Mellor-Yamada 2.5 closure scheme produces reasonable agreement to microstructure diffusivity measurements from the region [5].

The embedded lagrangian plume model within EFDC uses an integral control volume technique, tracking the radius, thickness, temperature, salinity, nutrient or dye concentration, and velocity at each plume element in the near-field. Entrainment is computed from both shear and forced entrainment (projected area entrainment). The model is coupled to the far-field using the Distributed Entrainment Sink Approach developed by Lee and Choi (2007) [6,7]. This method applies sink and source terms in the far-field domain based on the near-field plume entrainment and termination (respectively). In turn, the lagrangian plume model receives ambient conditions from the time-varying EFDC domain, providing a true two-way coupling between the near-field and far-field models without ad-hoc parameterizations.

C. Discharge Variables and Design Scenarios

Makai simulated 100MW OTEC plants with oceanographic design conditions selected from several years of Hawaii Regional ROMS hindcasts, representing typical and extreme conditions offshore of West O`ahu. The hindcast dataset includes flows and water properties that are forced by local barotropic tides, basin-scale flows, internal tides capable of producing significant thermocline fluctuations, and mesoscale

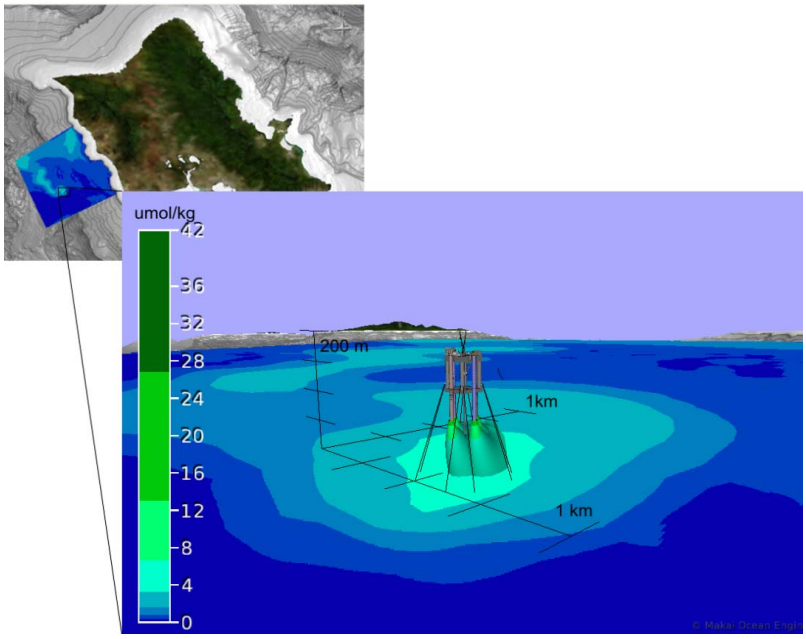

Fig. 1. Image of 100 MW OTEC plant with four 70 m, 1 m/s discharges, depicting the resultant plumes and nitrate (nutrient) concentration. The near-field plumes are the jets discharged from the OTEC plant, with a horizontal slice of the ocean shown at 130 m depth. The image was created with *Makai Voyager*.

eddies such as those that are periodically shed off the lee of the island of Hawai`i. Fig. 2 shows an example of the currents during the February and March 2008 hindcast used in our analysis. The period is characterized by a fluctuating background current with superimposed tidal flows and internal tides (seen as density fluctuations in the time series). Various OTEC plant configurations were also simulated to determine the properties and behavior of the near-field, intermediate-field, and far-field plumes as a function of the varying ambient conditions and discharge geometries. Discharge depth was varied from 70 to 100 meters, and discharge velocities were varied from 1 to 3 meters per second.

Plume dilution and spatial extent were analyzed with passive tracers, and the re-distribution of nitrate was modeled to give an estimate of the fate of biologically important nutrients. Nitrate and nitrite concentrations were obtained from Hawaii Ocean Time Series (HOTS) at Kahe Point, a monthly sampling station located off West O`ahu [8]. The HOTS data is shown in Fig. 3.

III. Results: Plume Behavior

1) Entrainment forced flows: Re-Circulation and Overshoot

Within the initial jet plumes, there is an input downward velocity of 1 to 3 m/s. The plumes lose vertical momentum as they entrain ambient water, and eventually reach the terminal depth with a vertical velocity of zero (by definition). Fig. 4 shows the vertical velocity in the jet-plumes and the far-field EFDC domain. As the jet-plumes sink they entrain large amounts of water from the surroundings, and subsequently redistribute it at the terminal depth of the plume. The far-field "sees" these plumes as a distribution of sinks along the plume trajectory, and as a source at the terminal depth. Table 1 shows an example of the distribution of these sources and sinks within the EFDC grid due to a 100 MW OTEC plume, with 420 m^3/s and 320 m^3/s of warm and cold water combined discharge, and an entrainment of nearly 9,000 m^3/s. This source-sink distribution forces a re-circulation, where upwelling occurs in a narrow vicinity around the jet-plumes. This is evident in Fig. 4, where there is an upward vertical velocity of about 0.14 m/s around the plumes, originating at the terminal depth and flowing upwards towards the distribution of entrainment sinks along the plume trajectory. The re-circulation is simulated in the CEROS plume model as an upward vertical velocity in the grid cells directly below the origin of the OTEC plant, with much weaker vertical velocities in the neighboring cells (which do not have large source-sink distributions since the jet-plume is primarily located directly below the OTEC plant). Thus the recirculation affects only a narrow region around the near-field plumes, and the far-field transport is still dictated by plume buoyancy and typical diffusion and advection processes of the ocean. However, this recirculation effect does contribute to increased near-field plume concentrations during periods with weak background flow, since the weaker horizontal currents allow more terminal plume waters to be re-circulated.

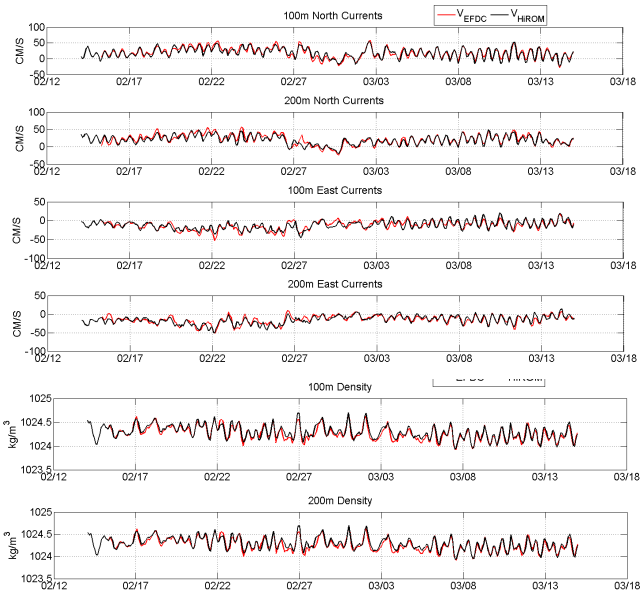

Fig. 2. Times series of North Currents, East Currents, and density at 100 meter and 200 meter depth from the OTEC Plume Model (red) and HI ROMS (black) taken at the center of the grid.

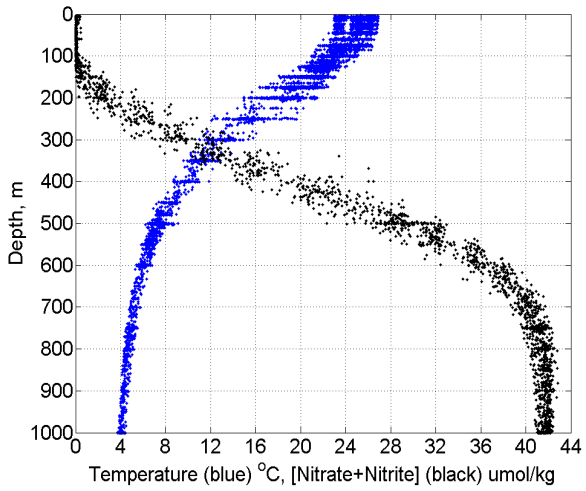

Fig. 3. Temperature (blue) and Nitrate (black) taken from the Hawaii Ocean Time Series (http://hahana.soest.hawaii.edu/hot/)

The process has been described in other large jet-plume systems and has been well studied with analytic and numerical techniques [9-11]. In addition, the excess momentum of the plumes can cause the near-field region to "overshoot" the equilibrium depth, causing an intense mixing zone around the terminal layer of the plume [12]. Both these processes result in the fact that sinking plumes entrain some of the terminal plume waters, rather than unmodified ambient water, affecting the terminal plume concentrations. The two-way coupling between the near-field and far-field model is critical to resolving these phenomena.

2) Effects of Current and Stratification

Stronger currents cause greater entrainment and dilution of the jet-plumes as they descend, which results in shallower but significantly more dilute plumes. An increased dilution with warm surface water causes the plumes to find equilibrium at shallower depths, but with significantly decreased concentrations compared to the periods with weak currents.

The dependence of the terminal plume depths to background current speeds and temperature was further quantified by regression analysis. A lowpass filter was applied to remove high frequency fluctuations to the time series of terminal jet-plume depths from a 70m 1m/s discharge, and the filtered data was correlated to the far-field temperature and currents near the OTEC plant. A maximum correlation was found to exist between the terminal jet-plume depth and the current and temperature at 120 meter in the water column. Similar correlation also existed between the equilibrium depth and surface temperatures, which is expected since surface waters account for 57% of the total discharge volume. More specifically, the terminal jet-plume depths show a correlation of 0.87 to the current magnitude at 120 meter depth, and a correlation of 0.38 to the temperature at 120 meter and at the surface. This suggests that the near-field plumes are strongly modified by the background currents, with less sensitivity to the changes in stratification and background temperatures.

This correlation between the current field and equilibrium depth of the near-field plume is shown in Fig. 5. The scatter plot shows background current magnitudes, resulting terminal depths, and bulk dilutions of the near-field plumes taken from a 30 day simulation during February and March, 2008 (each point in the fig. represents a 20 min interval, which coincides with the times the jet plume model is updated). When the currents are strong the plume is rapidly diluted with the surrounding (less dense) water, causing them to equilibrate at shallower depth. For example, currents of 60 cm/s produce plumes with a terminal depth of ~150 meter and a volumetric dilution ratio of ~20-30. Currents of 0-10 cm/s produce plumes with a terminal depth of ~200 meter and a volumetric dilution ratio of ~5.

The far field plume advection and dilution is also dominated by the background currents. Fig. 6 shows the resulting plume as a percentage of the original discharge concentrations at 110 to 170 m depth, based on a 100 MW OTEC plant discharging at 70 m depth and 1 m/s. During strong flow conditions the far-field plume is advected in long and narrow trajectories, and the plume can remain as narrow as 1-2 km as far as 10 km downstream. As seen in Fig. 6a, the plume has a narrow spatial pattern, with 16:1 dilution 5km downstream and a long, narrow tail that reaches 50:1 dilution 10km downstream. A 16:1 dilution occurs within 1km of the plant in all directions. During slack or weak flow conditions, the plume shows a greater tendency for radial dispersion at the equilibrium depth. From Fig. 6b, depicting slack (<10 cm/s) currents, a dilution of 10:1 is evident at a radial distance of 2 km from the OTEC plant and there exists a much shorter and wider plume "tail".

As discussed above, the stronger currents cause the plumes to entrain more water and equilibrate at shallower depths, but at lower nutrient concentrations. In contrast, during weak currents, when the plume is evidently largest in the horizontal scale and of higher concentration, it is also the deepest since it entrains less of the surrounding warmer water. This deepening of the plume when it is potentially of the highest concentration and size will help mitigate phytoplankton stimulation in the photic zone. Meanwhile, the stronger currents will also help

TABLE I. SOURCES AND SINKS IN GRID CELLS AT OTEC LOCATION DUE TO WARM WATER INTAKE, COLD WATER INTAKE, PLUME ENTRAINMENT, AND DISTRIBUTION OF PLUME AT THE TERMINAL DEPTH. POSITIVE VALUES ARE SOURCES IN THE FAR-FIELD, NEGATIVE VALUES ARE SINKS IN THE FAR-FIELD.

Depth (m)	Source/Sink (m^3/s)
-10	-420
-70	-438.8
-90	-2364
-110	-3093
-130	-2177
-150	8813
-1062	-320

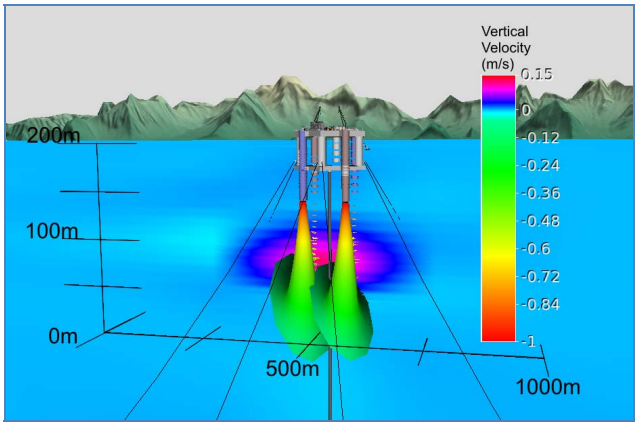

Fig. 4. Colormap of the vertical velocities in the jet-plumes and the far-field EFDC grid. Evident is the negative velocities of the jet-plumes, and some weak upward velocities in the immediate vicinity of the far-field. The vertical scale is exaggerated by a factor of 2. Results shown are from a 100 MW OTEC plant with 70 meter deep discharges and 740 m^3/s total flow.

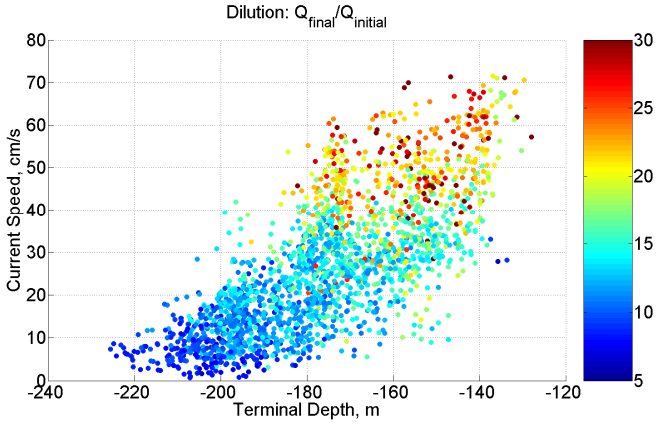

Fig. 5. Scatter plot showing terminal depth of sinking OTEC plumes simulated in the lagrangian jet-plume model vs background current speeds. The terminal depth and dilution is shown to be proportional to current. The result is shallower and less concentrated plumes during periods of strong flow.

mitigate phytoplankton stimulation by increasing the plume dilution, making the depth a less critical factor. Both cases have the effect of minimizing the potential for a phytoplankton bloom.

Fig. 7 shows three transects of the density field, temperature, tracer concentration, and nitrate concentration from a plume during a simulation time step having a slack current at the OTEC plant (<10cm/s). The path of the transect is shown in Fig. 6b as a dashed line. In Fig. 7 the tracer contours of the plume reach a depth of nearly 200 m directly below the plant, but remain at 150 m a few kilometers downstream. Further, the plume profile is relatively thick directly below the plant, with the iso-surface corresponding to a plume concentration of 10% (10:1 dilution) with a thickness of about 75 m. The temperature perturbation of the plume is also evident in fig. 7. At the equilibrium point of the near field plume (160 m depth and 2.2 km along the transect) the 18-19°C thermoclines becomes deeper and the 20-21°C thermoclines become shallower, indicative of the intense mixing and homogenized water column at the terminal depth. However, within less than 1 km of the plume center the thermoclines and pycnoclines return to normal, and the iso-surface corresponding to a dilution factor of 10:1 is quite thin. The plume reaches a dilution of 20:1 within 2 km downstream and at a depth of about 150 m. What is often simulated, and what is evident in Fig. 7 (taken during relatively slack currents of less than 10 cm/s), is that the excess momentum of the plume causes the plume to penetrate deeper than its neutral buoyancy layer. The plume, which is now positively buoyant, returns to a depth of about 150 m as it is wafted downstream. This phenomena, referred to as “fallback” or “overshoot”, is a well known feature of thermal plumes [12].

The discharge has an initial nitrate concentration of 18 umol/kg. Assuming a 10:1 dilution at 150 m depth (where ambient nitrate is ~2 umol/kg) we can expect the resultant nitrate levels to be about 3.5 umol/kg, just slightly above the ambient. As seen in Fig. 7c, the same area of the far-field plume characterized by a 10% concentration (10:1 dilution) shows about a 3 to 4 umol/kg nitrate concentration, and the nitrate and nitrite levels return to ambient values within a relatively close range of the OTEC plant.

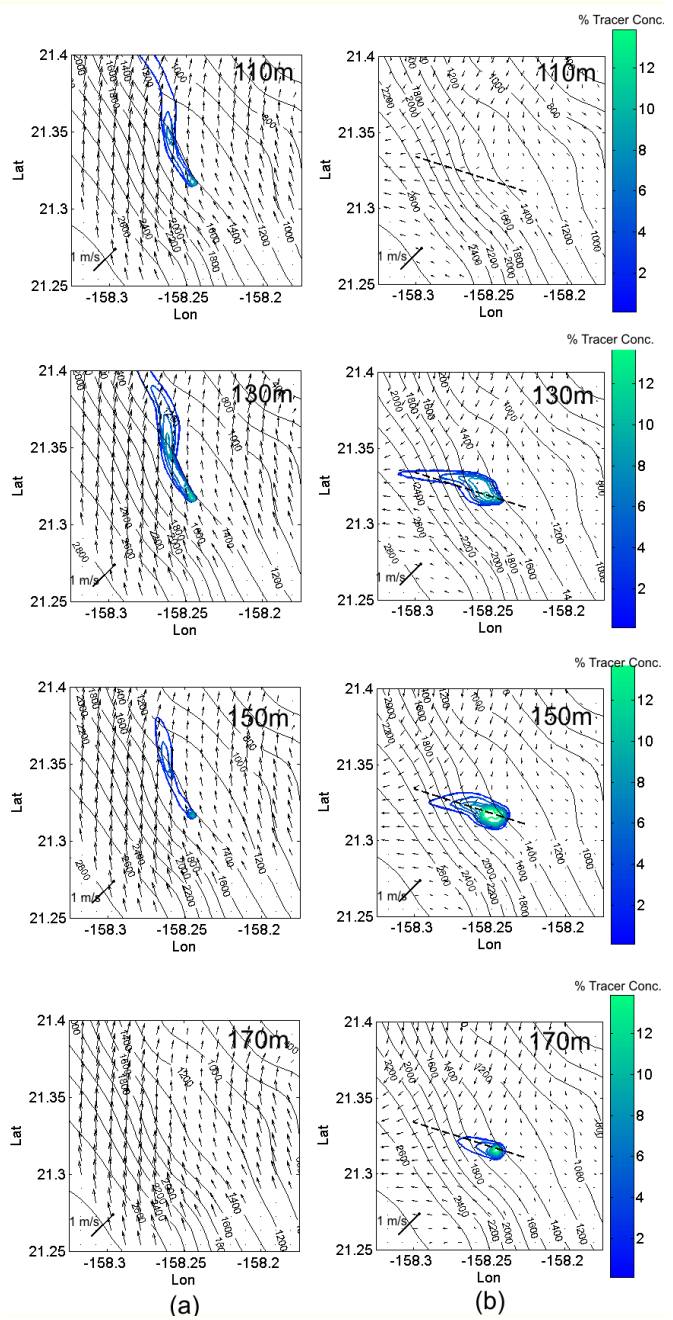

Fig. 6. (left column (a)) Slices of tracer concentration (% of original discharge concentration) and currents at 110 to 170 m depth, 1600, 19 Feb 2008, showing the fate of the plumes when currents are strong and to the northwest. (right column (b)) Slices of tracer concentration (% of original discharge concentration) and currents at 110 to 170 m depth, 1600, 29 Feb 2008, showing the fate of the plumes when currents are relatively weak near the OTEC plant and are directed to the west. A transect of the plume taken along the dashed line in (b) is shown in fig. 7.

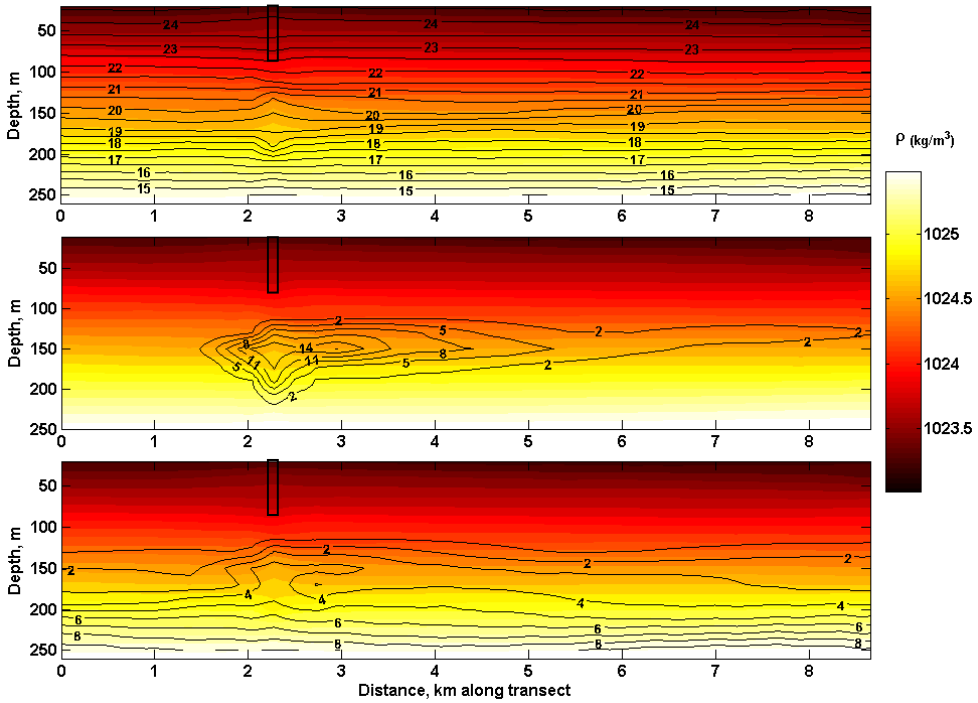

Fig. 7. (a, top) Transect of density (colored) and temperature contours (black lines) at intervals of 1.0°C (b, middle) Transect of density (colored) and plume concentration contours (black lines) at intervals of 3% ranging from 2 to 14% of the original discharge concentration. (c, bottom) Transect of density (colored) and nitrate contours (black lines), shown at 1µmol/kg intervals. Transects taken from simulation time step at 1600, 29 Feb 2008, during a period of relatively weak and convergent currents. The transect is shown as a dashed line in Fig. 6b, going from east to west. The location of the OTEC discharge pipes are depicted with the black rectangle at 2.2 km and 0 to 70 m depth.

IV. Results: Nutrient Distributions

A. *Single OTEC Plant*

OTEC discharges were simulated with discharge depth and outlet speeds of 70 m at 1 m/s, 70 m at 2 m/s, and 100 m at 1m/s in order to quantify the differences in the near-field and far-field plume depths and concentrations. Simulations were conducted using the February and March 2008 hindcast. Fig. 8 shows five averaged nutrient profiles from 50 to 225 meters deep, for the three different plant configurations, at varying distances upstream and downstream from a 100 MW OTEC plant. The profiles show nutrient data at locations 220m upstream, directly under the plant, and at 220, 880, and 1760 meters downstream. The colored solid lines show the average simulated nutrient profiles from the 30 day February-March simulation period, and colored dashed lines bound simulated nutrient levels that occurred 95% of the time. Gray zones indicate the 95% confidence interval of nutrient levels observed at the Hawaii Ocean Time Series station #2 near Kahe Point, Oahu, Hawai`i.

At the upstream location, the data show that observed nutrient levels with the OTEC plant are nearly the same as if no plant were present. Directly under the plant, the nutrient levels are noticeably elevated in the region from 70 m to 180 m deep. Here, the blue line representing the 100 m deep discharge (the highest cost option) is seen to cause the least nutrient perturbation.

At the location 220 m downstream, the average nutrient concentrations have been diluted so that at depths from 100 m to 150 m, the OTEC plume averages slightly exceed the 95% occurrence region for observed data. Nutrient levels are slightly elevated in the shallow region from 75 m to 100 m, and resume ambient levels at depths exceeding 180 meters.

By 880 meters downstream, the average nutrient levels from 75 m to 170 m deep remain elevated but are within the non-OTEC 95% occurrence region. For depths below 170 meters, the nutrient level is well within pre-OTEC observed ambient conditions. By 1760 m downstream, nutrient concentrations at all depths are within 0.5 µmol/l of non-OTEC conditions.

Overall, these data suggest that the zone of notable nutrient perturbation is bounded by the region from 70 m to 170 m deep, from less than 220 m upstream to 880 m downstream. The perturbed width is much narrower than the downstream distance, especially during above-average currents. During weaker currents, the zone of nutrient perturbation is somewhat less downstream and slightly wider transversely. A spatial view of the average resulting nitrate concentration from the 70 m, 1 m/s discharge is shown in Fig. 8.

Several additional months of simulations were run using the baseline 70 m, 1 m/s discharge, in order to investigate the seasonal changes in stratification, mesoscale eddy events, and other changes in the background circulation, the results of which are summarized in table 2. Due to overall stronger currents (25 cm/s compared to 13 cm/s), the near-field plumes

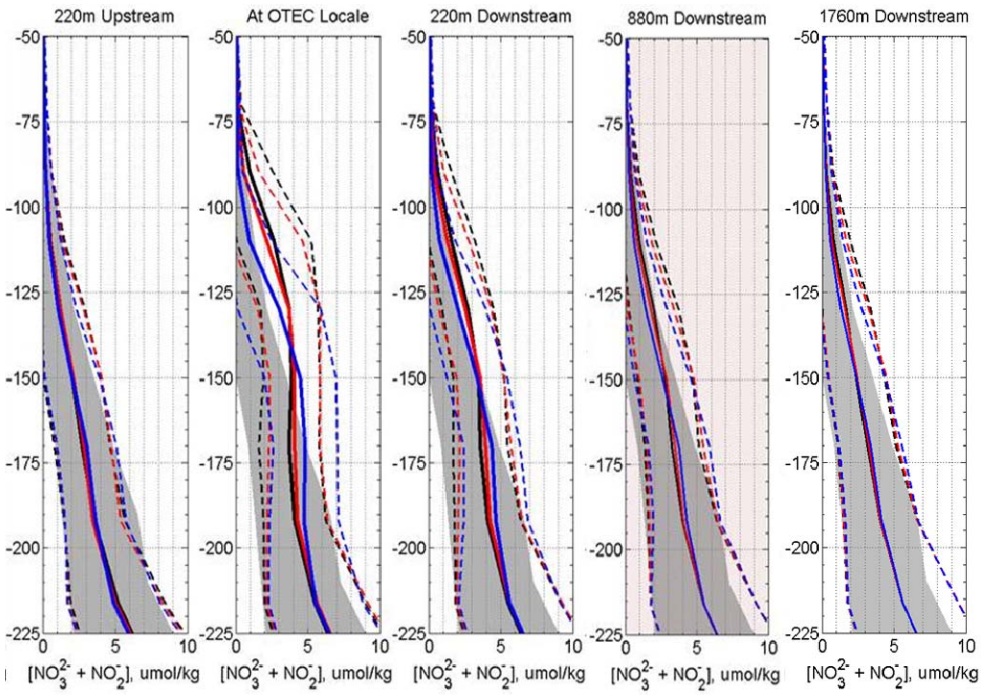

Fig. 8. Vertical nutrient profiles near an OTEC plant, compared with ambient nutrient profiles. The gray area shows the 95% confidence region of ambient nutrient levels observed at HOT Station 1, and is identical for each figure. The black, red and blue lines show three possible configurations of one 100MW OTEC plant, each during a 30-day simulation using Feb-Mar 2008 data. (Black: 1 m/s discharge speed at 70m deep, Red: 2 m/s at 70 m, and Blue: 1 m/s at 100 meter deep.) Solid lines show the 30 day average, dashed lines show ± 2σ (95%) confidence limits.

terminate at shallower depths with increased dilution (3.9 umol/kg vs 4.7 umol/kg nitrate) during our February-March simulation than either April-May or August-September. Also, the near-field plumes terminated slightly shallower during the August and September simulation than April and May, likely because this period was characterized by upper ocean temperatures that were ~1-2 °C warmer (average currents remained the same in both simulations).

B. Potential for Phytoplankton Stimulation

The primary environmental consideration when designing the discharge configuration is likely to be the potential for phytoplankton stimulation due to re-distribution of nutrients from deep, nutrient-rich water to shallow, nutrient-limited, waters. Discussion at the June 2010 NOAA OTEC Environmental Workshop focused on the desire to discharge at depths which are light-limited, so that phytoplankton stimulation would be inhibited. Makai has downloaded historical datasets from the Hawaii Ocean Time-Series Station 1 offshore Kahe Point in order to quantify the light-limited depth.

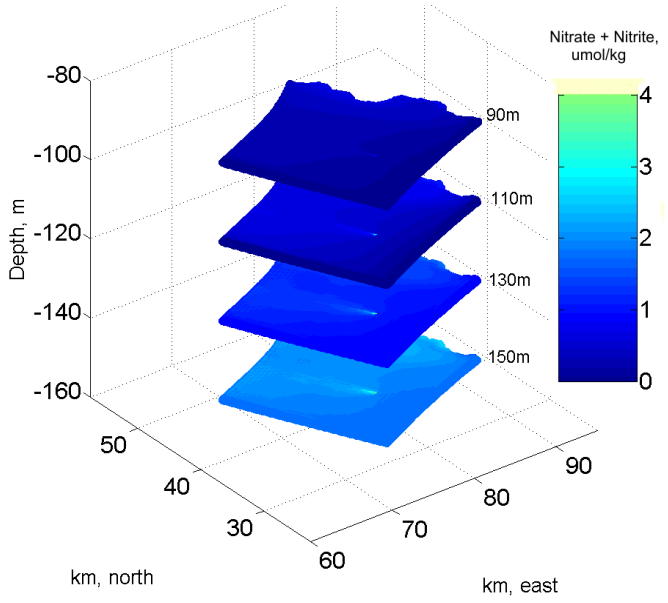

Fig. 9. Average Nitrate concentration during February and March 2008 from a 1 m/s 70 meter mixed discharge 100MW plant. Currents averaged 25 cm/s to the northwest at the OTEC site causing the plume to remain narrow and advect downstream.

TABLE II. AVERAGE CONDITIONS AND SIMULATED NEAR-FIELD PLUME PROPERTIES FOR FEBRUARY-MAR, APR-MAY, AND AUG-SEP FOR A 70 METER MIXED DISCHARGE AT 1 M/S. AVERAGE NITRATE CONCENTRATIONS ARE COMPUTED AT THE TERMINAL DEPTH OF THE JET PLUME.

Period	Avg Temp at Surface (°C)	Avg Temp at 100m (°C)	Avg Temp at 200m (°C)	Average Current at 120m Depth (m/s)	Average Equilbrium Depth (m)	Standard Deviation of Equlibrium Depth (m)	Average Plume Nitrate Concentration (μmol/kg)	HOT station 1 Nitrate at Equilibrium Depth (μmol/kg)
Feb-Mar	24.7	21.4	16.2	25	154	21.7	3.9	2 +/-2
Apr-May	24.2	21.3	16.9	13	176	18.5	4.7	3 +/-2
Aug-Sep	26.1	22.8	17.3	13	169	17.6	4.6	3 +/-2

Fig. 10 compares the Chlorophyll A and nitrate concentrations at Hawaii Ocean Time-Series Station #1 with the simulated nitrate concentrations from Makai's plume model. The observed chlorophyll maximum is at 100 meter depth, with some significant levels of chlorophyll found down to 150 m. The chlorophyll maximum depth is indicative of where phytoplankton growth becomes light limited. Below that level, additional nutrients needed for growth are available, but there is insufficient light for the majority of phytoplankton populations to grow. This data suggests that at depths below about 130 m, phytoplankton growth is light-limited rather than nutrient-limited, since excess nutrients are already present without being consumed. Thus, the HOTS data suggest that any OTEC-based nutrient enhancement below 130 meters depth will not cause significant phytoplankton stimulation.

C. Multiple OTEC Plants

Clusters of OTEC plants were simulated to investigate the possibility of downstream interactions of plumes with neighboring facilities. Results indicate that so far as the plants remain beyond the near-field region of neighboring discharges, there is minimal downstream effect. Fig. 11 shows the average nitrate concentrations directly below the OTEC plants as a result of 1.3 km and 3.3 km spaced sites. The nitrate levels are nearly identical at all three OTEC sites, regardless of their position. This result is not surprising, since we have already shown that the plumes will rapidly sink and approach ambient nitrate levels within 0.5 to 1 km of the plant. However, the same would not be true if the plumes interacted within the near-field range, which would require significantly less than 1km spacing. The dilution rate is much greater in the near-field jet-plumes (a dilution ratio of 10-20 as the jet-plume sinks), and entraining or diluting the near-field plume with waters that have higher ambient concentrations will significantly affect the concentration of that plume. This could have a pronounced affect on nitrate levels if a large number of OTEC plants were clustered with spacing of only a few hundred meters, and located downstream of one another. We have shown, however, that a spacing of 1.3 km provides enough distance for these interactions to become insignificant with regards to nitrate and nutrient loads because of the limited extent and rapid dilution of the near-field plumes.

Fig. 12 shows snapshots of the nitrate concentration and currents at 130 m depth at different times during the February-March simulation of 1.3 km spaced OTEC plants. As seen in Fig. 12a the plumes remain narrow and have very little interaction due to the relatively strong northwestward current. More interaction is evident in Fig. 12b, which is characterized by relatively weak and convergent currents around the OTEC cluster. However, the interaction does not cause a significant increase in the nitrate concentration, with no discernible difference between the upstream or downstream OTEC sites. Interestingly, Fig. 12 shows elevated background nitrate levels that are due to the ambient circulation (not the OTEC plumes), which reveals that the amount of natural variability that may be present in this system is similar in magnitude to the OTEC discharge plumes.

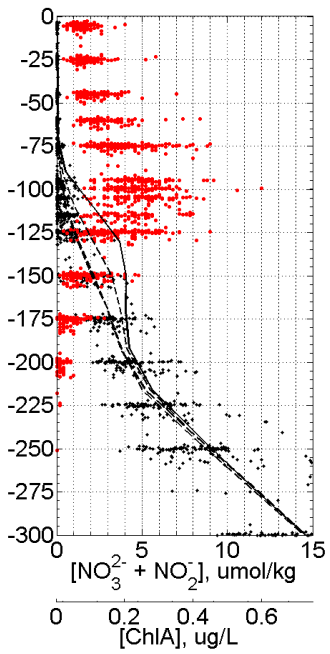

Fig. 10. Averaged profile of nitrate and nitrite (black dots) and chlorophyll A (red circles) from HOT station 1 with simulated nitrate concentrations under the OTEC plant (solid line) and at a radial distance of 440 meter from the OTEC plant (dashed lines). OTEC discharges were 2 m/s at 70 meter depth for a 100 MW capacity operation.

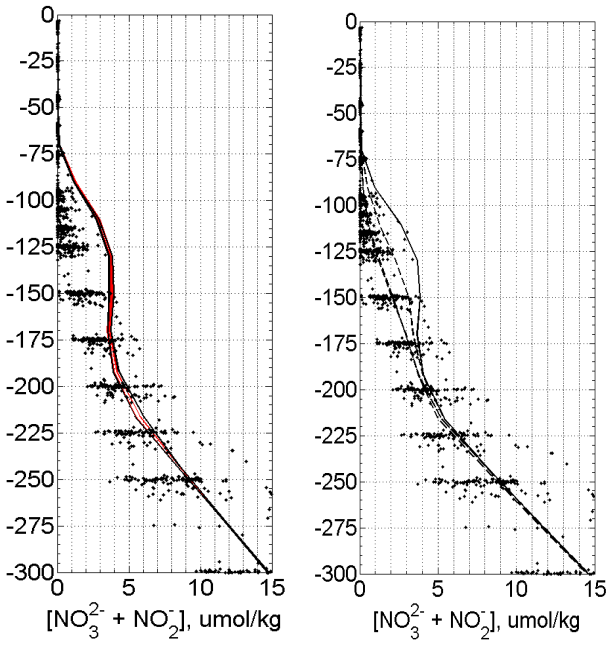

Fig. 11. Left: Average vertical profile of nitrate at the three OTEC plants spaced at distances of 1.3 km (red) and 3.3 km (black). Nitrate measurements from HOT station 1 at Kahe Point are also shown (black dots). Profiles at all three sites are plotted, but due to their close similarity it appears as if only two are plotted. Right: Average vertical profile of nitrate from the operation of a single OTEC directly below (solid) and at 440 m away (dashed). Again, all four grid cells at 440 m are plotted, but it appears as 2 due to the close similarity between the 3 upstream locations.

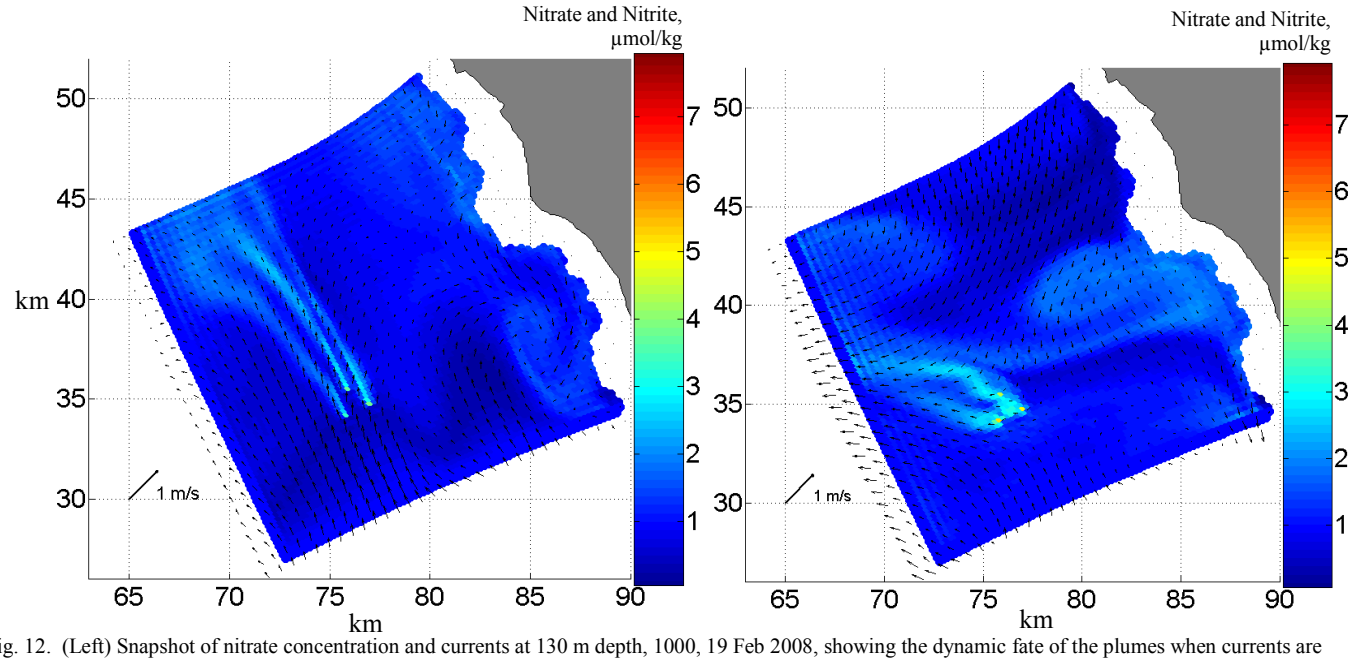

Fig. 12. (Left) Snapshot of nitrate concentration and currents at 130 m depth, 1000, 19 Feb 2008, showing the dynamic fate of the plumes when currents are strong and to the northwest.(Right) Snapshot of nitrate concentration and currents at 130 m depth, 1600, 29 Feb 2008, showing the dynamic fate of the plumes when currents are relatively weak near the OTEC plant and are directed to the west. (Color scale represents Nitrate and nitrate concentration in micromoles per kilogram of seawater)

V. Discussion

Makai Ocean Engineering has developed a 3-D hydrodynamic model of OTEC discharge plumes that simulate the dynamic near-field and far-field properties of OTEC plumes under realistic ocean conditions. The model, used in conjunction with the Hawaii Regional Ocean Model, permits OTEC engineers to select discharge system design parameters and quantify the environmental perturbation likely to occur.

A baseline environmental dataset exceeding one year was reviewed, and 120 days of representative output was developed from the HIROM model output to simulate the operation of OTEC plants under extreme and typical conditions while varying discharge configurations. The baseline dataset incorporated a large eddy event, winter and summer stratification, and periods with significant tidal and low frequency variability. It was determined that the dilution, trajectory, and terminal depths of the near field OTEC plumes were significantly affected by the background currents, and a clear trend was shown to exist. The strong flows increase the entrainment and mixing (dilution) rate in near-field plumes, resulting in shallower equilibrium depths, but less concentrated plumes. Stratification and the background temperature field was found to have a secondary effect compared to currents, with warmer waters in the upper water column resulting in slightly less dense plumes, which do not penetrate as deeply into the thermocline.

It was also shown that the plumes discharged at 70 or 100 meters deep with velocities of at least 1 m/s become diluted to naturally occurring nitrate levels within one kilometer downstream of an OTEC plant.

The model was expanded to simulate three 100MW OTEC plants spaced from 1.3 km to 3.3 km apart. It was shown that nitrate concentrations at the OTEC plants are unaffected by the presence of neighboring facilities, when spaced at least 1.3 km apart. Further, we showed that while plume interaction does occur in the far-field and downstream region of the OTEC clusters, it modifies the spatial extents of the plumes but does not create a discernible increase in nitrate concentration.

Comparisons with Hawaii Ocean Time Series data indicate that existing phytoplankton maximums occur at about 70-130 meter depth, at which point phytoplankton growth starts to become light limited and excess nutrients remain available. Any nutrient enhancement below 130 meters can be expected to provide only a very limited amount of phytoplankton stimulation. It is unlikely, based on the results of this study, that either the 70 meter 1 m/s, or 100 meter 1 m/s discharge would stimulate phytoplankton blooms (terminal plume depths of 154 meter and 174 meter respectively), due to both the rapid plume dilution that limits the horizontal extent (residence time) of nutrient enhancement as well as the lack of light at the far-field plume depth.

To continue this work, Makai has been awarded a Department of Energy grant to expand the simulations and include biochemical growth that may result from the plume. The ongoing project aims to quantify the phytoplankton response to the nutrient distribution presented here. In addition, the project includes funding to validate 7 months of hindcasts using current and CTD data collected during 2010 as part of a NAVFAC-sponsored effort. Makai is coordinating this modeling with biologists from the University of Hawaii and NOAA OTEC regulators, and is scheduled to finish in 2012.

ACKNOWLEDGMENT

The authors would like to thank the Defense Advanced Research Projects Agency (DARPA), the National Defense Center of Excellence for Research in Ocean Sciences (CEROS) for past funding that enabled development of the Makai CEROS OTEC Plume model. We would also like to thank the Department of Energy (DoE) for current funding under the Marine and Hydrokinetics Initiative to implement biological modeling. Additional technical support has been provided by Dr. John Hamrick of TetraTech, Inc. (author of EFDC) and Dr. Brian Powell of the University of Hawaii (Principal Investigator for Hawaii Regional ROMS model).

REFERENCES

[1] Myers, E.P., Hoss, D.E., Matsumoto, W.M., Peters, D.S., Seki, M. P., Uchida, R.N., Ditmars, J.D., Paddock., R.A. (1986) The Potential Impact of Ocean Therman Energy Conversion on Fisheries. NOAA Technical Report NMFS 40

[2] McAndrew, P. M., Bjorkam, K.M., Church, M/J/, Morris, P.J., Jachowski, N., Williams, P.J., Karl, D. (2007) Metabolic response of oligotrophic plankton communities to deep water nutrient enrichment, Marince Ecology Progress Series., 332, 63-75

[3] Hamrick, J.M., (1996): User's Manual for the Environmental Fluid Dynamics Computer Code, Special Report No. 331 in Applied Marine Science and Ocean Engineering, School of Marine Science, Virginia Institute of Marine Science, The College of William and Mary, Goucester Point, VA

[4] Powell, Brian. (2010) Personal correspondence (unpublished) with principal investigator for PacIOOS Hawaii Regional Ocean Model http://www.soest.hawaii.edu/pacioos/focus/modeling/roms.php

[5] Carter, G.S., Merrifield, M.A., Becker, J.M., Katsumata, K., Gregg, M.C., Luther, D.S., Levine, M.D., Boyd, T.J., Firing, Y.L. (2008). Energetics of M2 Barotropic-to Baroclinic Tidal Conversion at the Hawaiian Islands. *J. Phys. Oceanog.*, 28 2205-2223.

[6] Choi, K.W., Lee, J.H.W. (2007). Distributed Entrainment Sink Approach for Modeling Mixing and Transport in the Intermediate Field. *J. Hydraulic Eng.,* 133:7 804.

[7] Choi K.W., Mao, J.Q., Lee J.W. (2007) Real-time Hydro-environmental Modelling and Visualization System for Public Engagement: Technical Note on Validation of the 3D flow and mass transport model (EFDC/DESA). *University of Hong Kong.*

[8] Hawaii Ocean Time Series Interactive Access (HOT-DOGS) http://hahana.soest.hawaii.edu/hot/hot-dogs/interface.html

[9] Speer, K.G. (1989) A forced baroclinic vortex around a hydrothermal plume. *Geophysical Research Letters*. 16-5, 461-464.

[10] Lavelle, J.W., (1994) A convection model for hydrothermal plumes in a crossflow. *NOAA Technical Memorandum.* ERL PMEL-102

[11] McDonald, R.N. (1990) Far field flow forced by the entrainment of a convective plane plume in a rotating stratified fluid. *Journal Physical Oceanography*. 20, 1791-1798.

[12] List, E.J. (1982) Turbulent jets and plumes. *Ann. Rev. Fluid Mechanics.* 14, 189-212